PHYSICAL REVIEW A **94**, 022513 (2016)

Momentum distribution of positronium and its interactions with oxygen molecules studied by coincidence Doppler broadening spectroscopy

Yawei Zhou, Jingjing Li, Chongshan Yin, Wenfeng Mao, Juncheng Wang, and Chunqing He[*]
Key Laboratory of Nuclear Solid State Physics Hubei Province, School of Physics and Technology, Wuhan University, Wuhan 430072, China

(Received 3 May 2016; revised manuscript received 15 July 2016; published 29 August 2016)

The coincidence Doppler broadening (CDB) technique was applied to study the momentum distribution of positronium (Ps) and its interactions with oxygen molecules in free spaces of silica aerogels filled with nitrogen and oxygen mixtures of various ratios. The deconvoluted CDB spectra become narrower and narrower with increasing oxygen partial pressure, which is due to electron exchange collision of ortho-Ps (o-Ps) with oxygen molecules. The momentum distribution of para-Ps (p-Ps) was successfully derived from deconvoluted CDB spectra by a two-Gaussian-function fitting. The bimodal distribution of Ps momentum reveals that o-Ps atoms (with enough kinetic energy) can be moderated effectively by exciting oxygen molecules from the ground state to the excited state ($a'\Delta_g$ or $b'\Sigma_g{}^+$) through inelastic collisions. It is interesting to find that the energy difference ΔE between two components of p-Ps momentum distributions decreases gradually because more and more o-Ps atoms lose energy through elastic collisions prior to inelastic collisions as oxygen partial pressure increases.

DOI: 10.1103/PhysRevA.94.022513

I. INTRODUCTION

After being injected into condensed matter, an energetic positron e^+ slows down to thermal energy through collisions with atoms [1–4]. At the end of its track, e^+ either annihilates directly with an electron or forms an intermediate state, positronium (Ps) [5], a bound state of an electron and a positron. Ps is a unique atom that exists in two states: The antiparallel spin state with total spin $S = 0$ is called para-Ps (p-Ps) and the parallel spin state with total spin $S = 1$ is called ortho-Ps (o-Ps). In vacuum, p-Ps annihilates into 2γ rays with a mean lifetime of 1.25×10^{-10} s [6], while o-Ps annihilates into 3γ rays with a mean lifetime of 1.42×10^{-7} s [7]. Being only composed of leptons, Ps is a good atom to test quantum electrodynamics [8–11]. Recently, Cassidy and Mills reported that when intense positron bursts are implanted into a film of porous silica, Ps_2 is created on the internal pore surfaces [12]. Simultaneously, the interactions between Ps atoms in porous silica films were presented by using subnanosecond positron pulses and an improved detection system [13]. Nagashima *et al.* [14] have reported the thermalization process of positronium in silica-powder grains, aerogel grains, and gases studied by angular correlation of annihilation radiation (ACAR) and the momentum-transfer cross sections between Ps and gas molecules were estimated. Porous silica is an ideal medium for obtaining Ps atoms [15] for the investigation of the Ps quantum effect and the thermalization process of Ps in porous silica still is an interesting fundamental research topic.

In porous silica materials Ps atoms are efficiently formed (more than 50% of implanted positrons) [16] and they are emitted into the pores with kinetic energy [14,17]. Ps is formed in the pore wall (grains) where it generally has a short lifetime [15,18], but the Ps atoms that diffuse into internal pores have longer lifetime and may lose energy via collisions with the internal pore surfaces and/or gas molecules therein.

It is well known that o-Ps is quenched or converted into p-Ps and annihilates quickly in oxygen gas [19–22]. In general, such a process occurs through electron exchange collisions provided one or more electrons are unpaired in the oxygen molecule [21]. The ground state of the O_2 molecule is the triplet $X\,^3\Sigma_g^-$, where two of the outer electrons are unpaired and have parallel spins. The lowest and second lowest excited states are the singlets $a'\Delta_g$ and $b'\Sigma_g{}^+$, which correspond to 0.977 eV (E_a) and 1.62 eV (E_b) above the ground state, respectively. The possible mechanisms of the interactions between positronium and oxygen molecules are summarized in Table I [21,23]. Kakimoto *et al.* have reported the interactions between Ps and oxygen molecules by using an ACAR apparatus [22,23]. In the study of interactions between Ps and molecular gases, the ACAR measurements can be carried out with reasonable efficiency [14,24]. This method has been widely applied in studies of Ps formation, thermalization, and annihilation in gases [14,20,22–25].

The coincidence Doppler broadening (CDB) spectroscopy is a much simpler experimental setup with the advantages of a much faster data collection rate and a much weaker source requirement. As a positron and an electron annihilation, 2γ rays are emitted, the relative angle between the two photons is slightly less than π, and the energies of 2γ rays are Doppler shifted. From the measurement of either the distribution in a relative angle or the Doppler shift, information about the momentum distribution of the electrons can be obtained [26]. Lynn *et al.* have shown the advantage of using a two-detector setup in a study of thermal generation of vacancies in aluminum [26,27]. Recently, the CDB spectroscopy was successfully applied to study precipitates in alloys [28,29] and positron interaction with polar groups in polymers [30]. With a coincidence technique, the energy resolution of a CDB setup can be improved by a factor of $\sqrt{2}$ and the ratio of the positron annihilation peak to the background of a CDB spectrum can be increased up to $\sim 10^5$ [31]. The smearing effect of energy resolution of a Ge detector on the Doppler broadening spectrum can be further reduced by a deconvolution process [32–34] by using the ACARFIT program [35]. Details of the deconvolution process of CDB spectra can be found in the literature [36–38]. A proper data

---

[*] hecq@whu.edu.cn

TABLE I. Possible mechanisms of the interactions between positronium and oxygen molecules. Here D is an amplitude of nonexchange electron of positronium interaction with oxygen molecules, E is an amplitude of exchange an electron of positronium interaction with oxygen molecules, $a'\Delta_g$ is the first excitation state of oxygen molecules, $b'\Sigma_g{}^+$ is the second excitation state of oxygen molecules, E' is an amplitude that excites the ground electron of oxygen molecules to $a'\Delta_g$, and E'' is an amplitude that excites the ground electron of oxygen molecules to $b'\Sigma_g{}^+$ [21,23]. Obviously, these inelastic channels involving the excited states $a'\Delta_g$ and $b'\Sigma_g{}^+$ are open only when the kinetic energies of Ps are higher than E_a and E_b, respectively.

	Positronium interactions with oxygen molecules	Cross section	Annihilation
o-Ps	Elastic (nonconversion) scattering	$D^2+2DE+\frac{7}{3}E^2$	3γ
	Elastic conversion	$\frac{2}{3}E^2$	2γ
	Inelastic (nonconversion) scattering	$\frac{4}{3}E'^2\ (a'\Delta_g)$, $\frac{2}{3}E''^2\ (b'\Sigma_g{}^+)$	3γ
	Inelastic conversion	$\frac{2}{3}E'^2\ (a'\Delta_g)$, $\frac{1}{3}E''^2\ (b'\Sigma_g{}^+)$	2γ
p-Ps	Elastic (nonconversion) scattering	$(D+E)^2$	2γ
	Elastic conversion	$2E^2$	3γ
	Inelastic (nonconversion) scattering	forbidden	2γ
	Inelastic conversion	$2E'^2\ (a'\Delta_g)$, $E''^2\ (b'\Sigma_g{}^+)$	3γ

analysis method enables one to use CDB to obtain the Ps momentum distribution. In the present work, for simplicity we have used CDB spectroscopy to investigate the momentum distribution of p-Ps and interactions between Ps atoms and oxygen molecules in N_2 and O_2 mixtures.

II. EXPERIMENT

Silica aerogels with a density of 0.11 g/cm^3 (YI-30, with hydrophobic chemical groups on the grain surface, supplied by Panasonic Electric Works Co., Ltd.) were used as a medium for Ps atom formation. The Ps atoms, formed in porous silica aerogels, are emitted into free spaces of silica aerogels [39]. Ps with a few eV may also be created at the grain surface [14,17,40,41]. The experimental setup is shown schematically in Fig. 1. It consists of two parts: One is the gas mixing system used to adjust the flow ratio of N_2 and O_2 gases and the other is CDB spectroscopy. A 30 μCi ^{22}Na radioisotope, used as the positron source, was sandwiched by two blocks of silica aerogels and then sealed by aluminum foil. Experiments were operated at room temperature, the sample chamber was full of a mixture of O_2 and N_2 with a total pressure of 1 atm, and the oxygen partial pressure was adjusted from 0 to 1 atm. Each spectrum with at least 10^7 events was collected under various oxygen partial pressures. All the samples were stored in a desiccator before being used in the experiment.

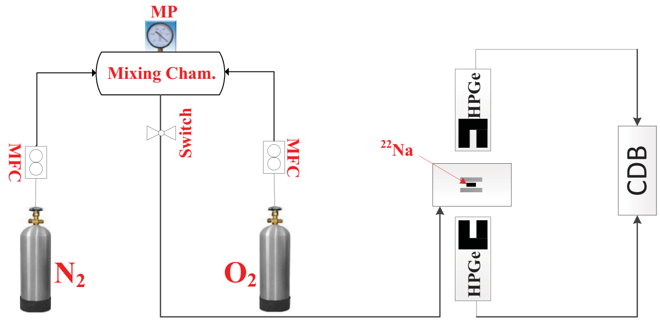

FIG. 1. Schematic diagram of the experimental setup, which is similar to that in our previous work [49].

Two high-purity germanium (HPGe) detectors were used for the CDB spectrum measurements and the energy resolution of each HPGe detector was 1.3 keV [full width at half maximum (FWHM)] at 511 keV. The energies of annihilating γ-ray pairs (denoted by $E_{1\gamma}$ and $E_{2\gamma}$) were simultaneously recorded by the two detectors located at an angle of 180° relative to each other. The energy difference between 2γ rays, $\Delta E_\gamma = E_{1\gamma} - E_{2\gamma}$, is expressed as cP_L and the sum of the energy $E_t = E_{1\gamma} + E_{2\gamma}$ is equal to the total energy of the electron-positron pair prior to annihilation, i.e., $2m_0c^2 - E_B$ (neglecting the thermal energies and chemical potentials), where P_L is the longitudinal component of the positron-electron momentum along the direction of the γ-ray emission, c is the speed of light, m_0 is the electron rest mass, and E_B is the Ps binding energy [31]. Selection of coincidence events that fulfill the condition $2m_0c^2 - 2.4\ \text{keV} < E_t < 2m_0c^2 + 2.4\ \text{keV}$ results in a significant improvement in the peak to background ratio (by three order of magnitude) over conventional one-detector measurement and as a result the variations of positron annihilation with different core electrons can be mapped. Figure 2 shows an original two-dimensional spectrum with at least 10^7 events recorded for two pieces of silica aerogel at 1.0 atm oxygen partial pressure. A detailed description of CDB spectroscopy can be found elsewhere [31]. Since the self-annihilation of p-Ps contributes a narrow peak to the CDB spectrum because of its almost zero momentum, it might be possible to derive the p-Ps momentum distribution by utilizing a multi-Gaussian-function fitting [42–44] of Doppler broadening spectrum using the ACARFIT program [35]. An enhanced energy resolution of ~0.92 keV at 511 keV, corresponding to $3.59 \times 10^{-3} m_0c$ for momentum resolution, was applied for the deconvolution process.

III. RESULTS AND DISCUSSION

Figure 3 shows the deconvoluted CDB spectrum of YI-30 in various oxygen partial pressures. All CDB spectra are normalized to the same total counts and could be well described

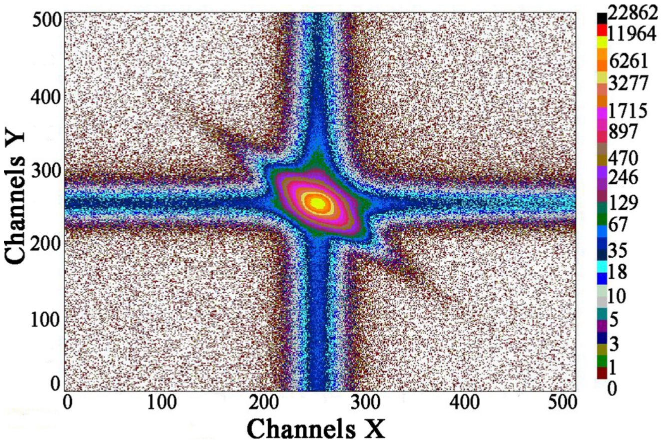

FIG. 2. Original two-dimensional display of the coincident events collected with at least 10^7 counts at 1.0 atm oxygen partial pressure.

by a wide component and a narrow one. It can be seen that the narrow component shows a remarkable increment as oxygen partial pressure increases, while the broad one declines along with the increase of oxygen partial pressure, which represents the free positron annihilation and pickoff annihilation of o-Ps atoms [23,45]. The narrow component seems to contain a lower momentum component with shoulders. The narrow component may correspond to the p-Ps annihilation [46]. Narrowing of the peak width can be attributed to the contribution from the conversion of o-Ps into p-Ps through electron exchange collisions with oxygen molecules. Thus, the tendency of the curves indicates that the oxygen molecule plays a significant role in the Ps atom quenching process. As the oxygen partial pressure increases, the p-Ps signal is enhanced and the o-Ps signal is on the wane, i.e., o-Ps + O_2 → p-Ps + O_2 → 2γ + O_2 (spin conversion) [19,20].

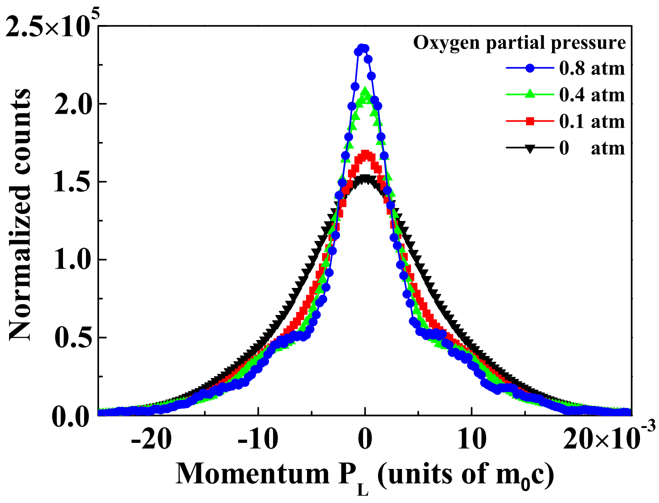

FIG. 3. Deconvoluted CDB spectra in YI-30 (top to bottom) corresponding to oxygen partial pressures of 0.8, 0.4, 0.1, and 0 atm, respectively.

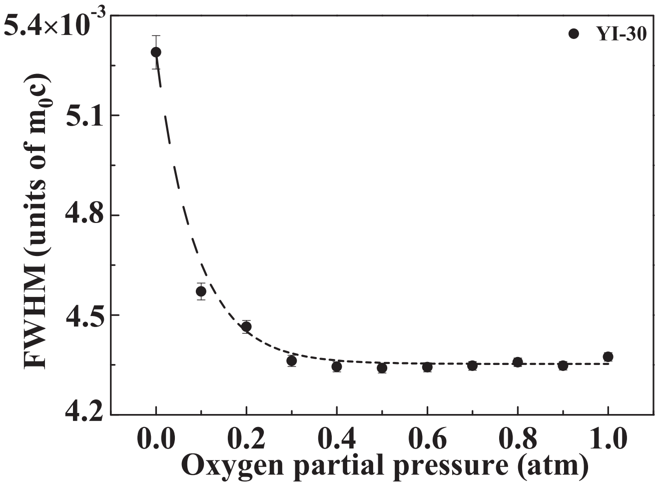

FIG. 4. The FWHM of the narrow component in YI-30 as a function of oxygen partial pressure.

In order to further understand the role of the oxygen molecule in the collision process, the FWHM of the narrowest component of the CDB spectrum of YI-30 with various oxygen partial pressures has been obtained using the ACAFIT program [35], as shown in Fig. 4. The energy axis (y axis) is expressed in momentum in units of $10^{-3} m_0 c$. As oxygen is introduced, the collision between o-Ps and O_2 molecules leads to the thermalization of o-Ps. In addition, o-Ps turns into p-Ps through spin exchange conversion [19,20], which results in a sharp decrement of the FWHM of the narrow component, while the FWHM remains unchanged with oxygen partial pressure increasing from 0.4 atm to 1.0 atm in YI-30. These results indicate that the major energy loss of p-Ps is dominated by inelastic collisions between Ps atoms with oxygen molecules, which is associated with the excitation energy of the O_2 molecule, and as oxygen partial pressure further increases, the Ps atoms with limited energy can only interact with oxygen molecules through elastic collision and then annihilate into 2γ rays.

As mentioned above, the interaction between Ps and oxygen molecules includes inelastic and elastic collisions. The narrow momentum distribution of p-Ps in oxygen can be obtained from a CDB spectrum with a total count of 10^7, based on the equation [23]

$$F(p) = -2p\frac{d}{dp}[N(p) - B(p)], \tag{1}$$

where $N(p)$ denotes the corresponding whole CDB spectroscopy and $B(p)$ denotes the Gaussian broad component. The momentum distribution of $F(p)$ at 0 atm can be approximated as the original p-Ps atoms at the instant of their annihilation, because the Ps energy loss in N_2 is negligible due to the elastic collision between Ps and N_2 molecules [47,48]. The p-Ps kinetic energy loss per collision with the grain surface is approximately 10^{-4} of the energy of p-Ps at the time of collision (depending on the effective mass of silica surfaces) [14,40] and there are several hundred collisions in the present aerogels during the short lifetime of p-Ps. Therefore, the part of the energy loss in N_2 before p-Ps annihilation is only

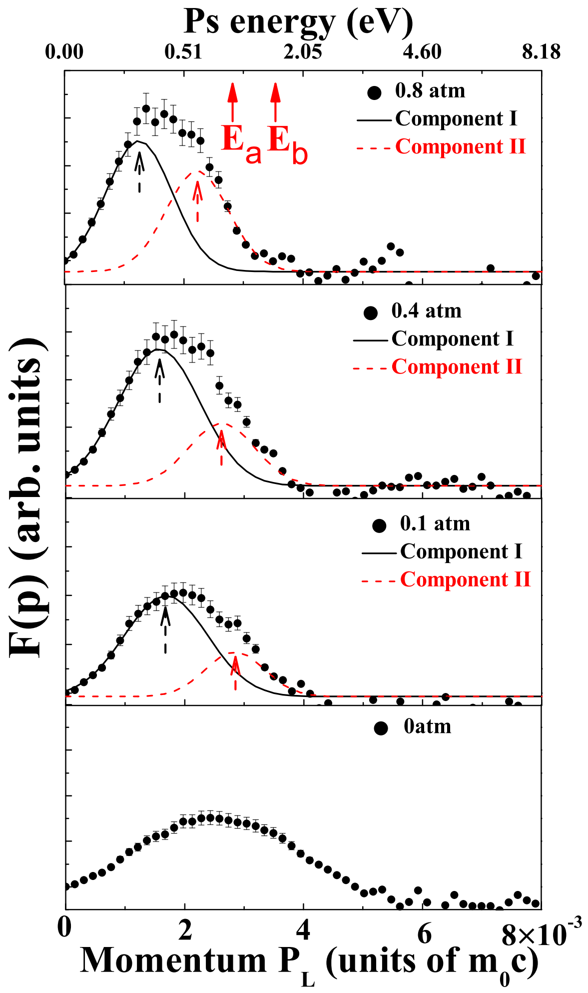

FIG. 5. Momentum distribution of positronium in YI-30 at various oxygen partial pressures. All the spectra are normalized to the same total count. The solid arrows indicate the Ps momenta corresponding to kinetic energies equal to E_a (0.977 eV) and E_b (1.62 eV), respectively. The dashed arrows indicate the peak positions at different oxygen partial pressures.

a few percent of its initial energy. The effects on the short-lived p-Ps in N_2 and in vacuum are comparable to each other [23]. Hence, within acceptable error, $F(p)$ in N_2 can be regarded as the initial momentum distribution of the p-Ps atoms emitted from the silica aerogel.

In the presence of O_2, based on Eq. (1), the momentum distribution of p-Ps in YI-30 is obtained at various oxygen partial pressures as shown in Fig. 5. The first and second excitation energies of the O_2 molecule, E_a and E_b, are indicated in the figure by arrows. The curve of the momentum distribution of p-Ps in nitrogen gas is symmetric. However, as oxygen gas is introduced, the curves are shifted in the low-energy direction, while they become more asymmetric and show a small peak in the high-energy direction. Hence, the momentum distribution of p-Ps in oxygen is decomposed into two components based on the two-Gaussian-function fitting. The intensities of both components increase as oxygen partial pressure increases; in particular, the intensity of component II is enhanced significantly. This result indicates that the amount of p-Ps annihilation increases as oxygen partial pressure increases due to o-Ps conversion. A slight change is found in the peak position of component I with increasing oxygen partial pressure, whereas the peak position of component II shifts to low energy significantly and both distributions become much narrower. The energy difference ΔE between two components obtained at various oxygen partial pressures is shown in Fig. 6. It is worth noting that the energy difference ΔE between two components at a low oxygen partial pressure of 0.1 atm is approximately equal to the energy gaps E_b and E_a within acceptable error, i.e., $\Delta E \approx E_b - E_a$. Interestingly, ΔE becomes smaller and smaller as oxygen partial pressure increases; a similar result could be found in the literature [23].

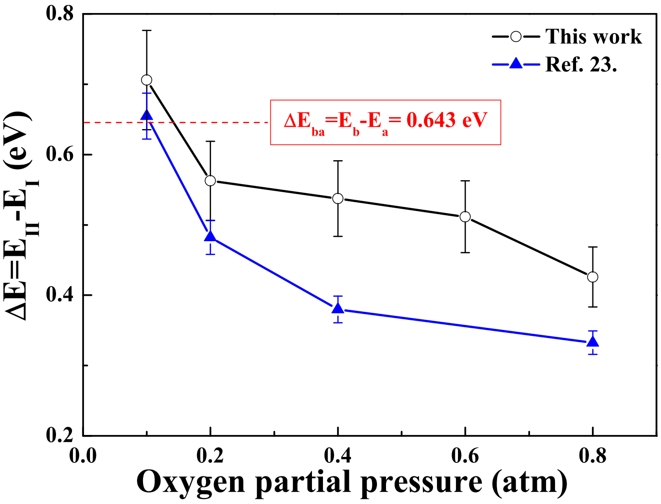

FIG. 6. Variations of the energy difference ΔE between two components at various oxygen partial pressures. Here E_I and E_{II} represent the energy of peak position of components I and II, respectively. Open circles and closed triangles refer to measurements in this work and [23], respectively.

In a previous paper [45] Zhang *et al.* obtained the cross section for the o-Ps inelastic collision with oxygen molecules through different processes. The cross sections of o-Ps conversion σ_{o-p} are dependent on the inelastic collision process as

$$\sigma_{o-p}(E_b) \sim 2.1 \times 10^{-17}\ \text{cm}^2$$
$$\sigma_{o-p}(E_a) \sim 6.6 \times 10^{-18}\ \text{cm}^2. \tag{2}$$

where $\sigma_{o-p}(E_b)$ and $\sigma_{o-p}(E_a)$ represent the conversion cross sections of o-Ps by exciting the O_2 molecule from the ground state to the $b'\Sigma_g{}^+$ and $a'\Delta_g$ states at 0.2 atm oxygen partial pressure, respectively. In our previous work [49], the elastic cross section of o-Ps quenching obtained is $\sim(1.37 \pm 0.05) \times 10^{-19}$ cm^2 at 1.0 atm oxygen partial pressure, which is much smaller than the cross section of the inelastic collision. Therefore, the o-Ps atoms lose most of their energy through inelastic collision, especially at low oxygen partial pressure. It is observed that the intensity of component I is higher than that of component II. Taking into account the cross section of different collision processes, this result indicates that the components I and II of the p-Ps momentum distribution might be due to o-Ps slowing down by exciting O_2 molecules from the ground state to the excited states $b'\Sigma_g{}^+$ and $a'\Delta_g$, respectively.

As shown in Fig. 6, the energy difference ΔE between two components decreases as a function of oxygen partial pressure. This could be due to the o-Ps atom energy loss through elastic collision, during which the o-Ps atoms with enough energy [14,17,40] would interact with O_2 molecules by exciting them from the ground state to the excited state ($a'\Delta_g$ or $b'\Sigma_g{}^+$). The probability of the inelastic collision depends on the cross section of the collision process. Indeed, the energy difference ΔE between two components at a low oxygen partial pressure of 0.1 atm is essentially equal to energy gaps of E_b and E_a, i.e., $\Delta E \approx E_b - E_a$. Considering such a fact and the collision cross-section dependence of the Ps momentum distribution shown above, it is likely that components I and II result from the conversion of o-Ps to p-Ps by exciting the O_2 molecule from the ground state to the excited states $b'\Sigma_g{}^+$ and $a'\Delta_g$, respectively. The present result also indicates that the initial energy of o-Ps emitted from such a hydrophobic silica aerogel could be ~2 eV, which agrees well with the emission energy of Ps from the hydrophobic porous silica measured by the Ps time of flight [40]. Thus, the emission energy of Ps from the silica surface depends on local physicochemical environments of silica, for instance, the pore and/or grain surface chemistry [17,40]. Prior to inelastic collision, o-Ps atoms might have experienced numerous elastic collisions. As the oxygen partial pressure further increases, the o-Ps atoms have higher probability to interact with oxygen molecules through elastic collision, which results in the peak positions of two components gradually shifting to the low-energy direction, especially the peak position of component II, as mentioned above. Thus, the energy difference ΔE between two components becomes smaller and smaller as the oxygen partial pressure increases. Further, because of the o-Ps slowing down by elastic collision, more and more o-Ps atoms with limited energy can only excite O_2 molecules to the $a'\Delta_g$ state. This could explain the distinct increment in the intensity of component II as the oxygen partial pressure increases. Hence, the o-Ps atoms lose energy through inelastic collision at low oxygen partial pressure, because of the larger cross section of the inelastic collision, while as the oxygen partial pressure further increases, the o-Ps atoms have higher probability to lose energy through elastic collision with oxygen molecules. One should keep in mind that although the conversion of p-Ps into o-Ps might occur, the conversion rate is very low because of the high annihilation rate of p-Ps. Although the energy difference ΔE in this work is slightly higher than those derived from the study by ACAR [23], considering the much lower energy resolution of CDB spectroscopy, the present results are quite acceptable and clearly demonstrate that both inelastic and elastic collisions play an important role in the interaction process between Ps atoms and oxygen molecules.

IV. CONCLUSION

In summery, instead of using angular correlation of annihilation radiation, coincidence Doppler broadening spectroscopy has been used as a quite simple measurement to obtain the momentum distribution of p-Ps and to study the interaction process between o-Ps atoms and oxygen molecules. The deconvoluted CDB spectra become narrower and narrower as oxygen partial pressure increases, which results from the conversion of o-Ps to p-Ps through electron exchange collisions with oxygen molecules. As oxygen is introduced, the FWHM decreases significantly and then the FWHM remains unchanged as oxygen partial pressure further increases. These results indicate that p-Ps atoms lose energy through inelastic collision as well as elastic collision. The momentum distributions of p-Ps were successfully derived from deconvoluted CDB spectra by two-Gaussian-function fitting. Component I mainly results from o-Ps atoms losing energy through exciting the oxygen molecule from the ground state to the second excited state $b'\Sigma_g{}^+$ and being converted to p-Ps atoms; then it does not lose much energy because of its short lifetime (~125 ps). In contrast, because of the small collision cross section, component II results from o-Ps atoms losing energy by exciting the oxygen molecule from the ground state to the first excited state $a'\Delta_g$. The energy difference ΔE between two components decrease gradually as the oxygen partial pressure increases; this indicated that before the inelastic collision process o-Ps atoms were thermalized through elastic collision with oxygen molecules.

ACKNOWLEDGMENTS

This work was supported by the National Natural Science Foundation of China through Grants No. 11575130 and No. 11375132 and the Research Foundation of Wuhan University (China) through Grant No. 2042015kf0190.

---

[1] M. R. Natisin, J. R. Danielson, and C. M. Surko, J. Phys. B **47**, 225209 (2014).
[2] R. M. Nieminen and J. Oliva, Phys. Rev. B **22**, 2226 (1980).
[3] J. Oliva, Phys. Rev. B **21**, 4909 (1980).
[4] J. Oliva, Phys. Rev. B **21**, 4925 (1980).
[5] A. Rich, Rev. Mod. Phys. **53**, 127 (1981).
[6] A. H. Al-Ramadhan and D. W. Gidley, Phys. Rev. Lett. **72**, 1632 (1994).
[7] R. S. Vallery, P. W. Zitzewitz, and D. W. Gidley, Phys. Rev. Lett. **90**, 203402 (2003).
[8] K. Danzmann, M. S. Fee, and S. Chu, Phys. Rev. A **39**, 6072 (1989).
[9] A. P. Mills, Jr. and G. H. Bearman, Phys. Rev. Lett. **34**, 246 (1974).
[10] S. Chu and A. P. Mills, Jr., Phys. Rev. Lett. **48**, 1333 (1982).
[11] G. S. Adkins, R. N. Fell, and J. Sapirstein, Ann. Phys. (NY) **295**, 136 (2002).
[12] D. B. Cassidy and A. P. Mills, Jr., Nature (London) **449**, 195 (2007).

[13] D. B. Cassidy and A. P. Mills, Jr., Phys. Rev. Lett. **100**, 013401 (2008).
[14] Y. Nagashima, M. Kakimoto, T. Hyodo, K. Fujiwara, A. Ichimura, T. Chang, J. Deng, T. Akahane, T. Chiba, K. Suzuki, B. T. A. McKee, and A. T. Stewart, Phys. Rev. A **52**, 258 (1995).
[15] D. W. Gidley, W. E. Frieze, T. L. Dull, A. F. Yee, E. T. Ryan, and H.-M. Ho, Phys. Rev. B **60**, R5157(R) (1999).
[16] M. P. Petkov, C. L. Wang, M. H. Weber, K. G. Lynn, and K. P. Rodbell, J. Phys. Chem. B **107**, 2725 (2003).
[17] Y. Nagashima, Y. Morinaka, T. Kurihara, Y. Nagai, T. Hyodo, T. Shidara, and K. Nakahara, Phys. Rev. B **58**, 12676 (1998).
[18] C. He, M. Muramatsu, T. Ohdaira, N. Oshima, A. Kinomura, R. Suzuki, and Y. Kobayashi, Radiat. Phys. Chem. **76**, 204 (2007).
[19] K. Wada, F. Saito, and T. Hyodo, Phys. Status Solidi C **6**, 2510 (2009).
[20] N. Shinohara, N. Suzuki, T. Chang, and T. Hyodo, Phys. Rev. A **64**, 042702 (2001).
[21] R. A. Ferrell, Phys. Rev. **110**, 1355 (1958).
[22] M. Kakimoto, T. Hyodo, and T. B. Chang, J. Phys. B **23**, 589 (1990).
[23] M. Kakimoto, T. Hyodo, T. Chiba, T. Akahane, and T. B. Chang, J. Phys. B **20**, L107 (1987).
[24] Y. Nagashima, T. Hyodo, K. Fujiwara, and A. Ichimura, J. Phys. B **31**, 329 (1998).
[25] M. Kakimoto and T. Hyodo, J. Phys. B **21**, 2977 (1988).
[26] K. G. Lynn, J. R. MacDonald, R. A. Boie, L. C. Feldman, J. D. Gabbe, M. F. Robbins, E. Bonderup, and J. Golovchenko, Phys. Rev. Lett. **38**, 241 (1977).
[27] K. G. Lynn, J. E. Dickman, W. L. Brown, M. F. Robbins, and E. Bonderup, Phys. Rev. B **20**, 3566 (1979).
[28] T. Onitsuka, M. Takenaka, E. Kuramoto, Y. Nagai, and M. Hasegawa, Phys. Rev. B **65**, 012204 (2001).
[29] Y. Nagai, K. Takadate, Z. Tang, H. Ohkubo, H. Sunaga, H. Takizawa, and M. Hasegawa, Phys. Rev. B **67**, 224202 (2003).
[30] Y. Nagai, T. Nonaka, M. Hasegawa, Y. Kobayashi, C. L. Wang, W. Zheng, and C. Zhang, Phys. Rev. B **60**, 11863 (1999).
[31] P. Asoka-Kumar, M. Alatalo, V. J. Ghosh, A. C. Kruseman, B. Nielsen, and K. G. Lynn, Phys. Rev. Lett. **77**, 2097 (1996).
[32] S. Dannefaer and D. Kerr, Nucl. Instrum. Methods **131**, 119 (1975).
[33] T. Chang, M. Xu, and X. Zeng, Phys. Lett. A **126**, 189 (1987).
[34] H. J. Zhang, Z. Q. Chen, S. J. Wang, A. Kawasuso, and N. Morishita, Phys. Rev. B **82**, 035439 (2010).
[35] P. Kirkegaard, M. Eldrup, O. E. Mogensen, and N. J. Pedersen, Comput. Phys. Commun. **23**, 307 (1981).
[36] J. D. Zhang, T. J. Zhou, C. K. Cheung, C. D. Beling, S. Fung, and M. K. Ng, Nucl. Instrum. Methods Phys. Res. Sect. A **560**, 552 (2006).
[37] M. Morháč, Nucl. Instrum. Methods Phys. Res. Sect. A **559**, 119 (2006).
[38] M. Morháč and V. Matoušek, J. Comput. Appl. Math. **235**, 1629 (2011).
[39] T. B. Chang, J. K. Deng, T. Akahane, T. Chiba, M. Kakimoto, and T. Hyodo, in *Positron Annihilation*, edited by P. C. Jain, R. M. Singru, and K. P. Gopinathan (World Scientific, Singapore, 1985).
[40] C. Q. He, T. Ohdaira, N. Oshima, M. Muramatsu, A. Kinomura, R. Suzuki, T. Oka, and Y. Kobayashi, Phys. Rev. B **75**, 195404 (2007).
[41] C. Q. He, S. J. Wang, Y. Kobayashi, T. Ohdaira, and R. Suzuki, Phys. Rev. B **86**, 075415 (2012).
[42] G. Dlubek, H. M. Fretwell, and M. A. Alam, Macromolecules **33**, 187 (2000).
[43] A. Alba Garcia, L. D. A. Siebbeles, A. Rivera, H. Schut, S. W. H. Eijt, R. Escobar Galindo, and A. van Veen, Mater. Sci. Forum **363-365**, 287 (2001).
[44] Z. Q. Chen, M. Maekawa, S. Yamamoto, A. Kawasuso, X. L. Yuan, T. Sekiguchi, R. Suzuki, and T. Ohdaira, Phys. Rev. B **69**, 035210 (2004).
[45] T. B. Zhang and M. Xu, High Energy Phys. Nucl. Phys. **14**, 289 (1990).
[46] H. J. Zhang, Z. Q. Chen, and S. J. Wang, J. Chem. Phys. **136**, 034701 (2012).
[47] M. Skalsey, J. J. Engbrecht, R. K. Bithell, R. S. Vallery, and D. W. Gidley, Phys. Rev. Lett. **80**, 3727 (1998).
[48] M. Skalsey, J. J. Engbrecht, C. M. Nakamura, R. S. Vallery, and D. W. Gidley, Phys. Rev. A **67**, 022504 (2003).
[49] Y. W. Zhou, W. F. Mao, Q. C. Li, J. C. Wang, and C. Q. He, Chem. Phys. **459**, 81 (2015).